The Egyptian Journal of Remote Sensing and Space Sciences (2016) xxx, xxx–xxx

HOSTED BY

National Authority for Remote Sensing and Space Sciences

The Egyptian Journal of Remote Sensing and Space Sciences

www.elsevier.com/locate/ejrs
www.sciencedirect.com

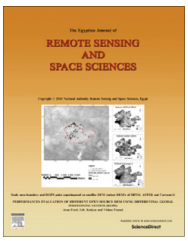

RESEARCH PAPER

# Contribution of remote sensing techniques to the recognition of titanite occurrences at Gabal El-Degheimi area, Central Eastern Desert, Egypt

**Ahmed E. Khalil** [a], **Hatem M. El-Desoky** [b], **Salem S.M.** [c,*]

[a] *Department of Geology, National Research Center, Egypt*
[b] *Department of Geology, Faculty of Science, Al-Azhar University, Egypt*
[c] *National Authority for Remote Sensing and Space Sciences, Egypt*

Received 29 December 2015; revised 8 June 2016; accepted 7 August 2016

**KEYWORDS**

Titanite;
Volcaniclastic;
Remote sensing

**Abstract** The present study aims at delimiting the titanite occurrences in the volcaniclastic metasediments and accessing the mineral chemistry of the titanite at Gabal El-Degheimi area. The study area is a part of the Arabian Nubian shield and includes serpentinites, arc volcaniclastic metasediments, older granites, Dokhan volcanics, Hammamat group post orogenic volcanics and younger granites. The processing of Landsat 8 images, field geological verification and geochemical analyses highlighted the distribution and occurrences of the arc volcaniclastic metasediments and their included alteration zones all over the study area. These rocks are composed of titanite, chlorite, calcite, epidote, sericite, muscovite and biotite in trace amounts, about 3 wt% of $TiO_2$ was recorded. Titanite mineral is the main carrier of titanium, calcium and silicon in the volcaniclastic metasediments.



## 1. Introduction

The study area is located in the Central Eastern Desert between latitude 25°57′–26°02′ N and longitude 33°55′–34°02′ E, covering an area of about 60 $km^2$ (Fig. 1). The Central Eastern Desert of Egypt is a part of the Pan African Arabian-Nubian Shield (ANS) that was discussed and described by many authors as displaying a tectonized regime involving complicated geologic processes producing mineralizing fluids that were sources for ore deposition when expelled from the deeper parts of an orogen (Oliver, 1986; Nesbitt, 1992; Garven et al., 1999). Johnson et al. (2011) studied the history of the ANS with respect to the depositional plutonic structural and tectonic events associated with the closing stages of the northern East African orogen. The Central Eastern Desert is known for its numerous ore mineral occurrences as it includes a variety of geological environments favorable to mineral ore formation. Each rock or rock assemblage charac-

* Corresponding author.
E-mail address: salem_moher@hotmail.com (S.M. Salem).

Peer review under responsibility of National Authority for Remote Sensing and Space Sciences.

http://dx.doi.org/10.1016/j.ejrs.2016.08.003
1110-9823 Production and hosting by Elsevier B.V. on behalf of National Authority for Remote Sensing and Space Sciences.


Please cite this article in press as: Khalil, A.E. et al., Contribution of remote sensing techniques to the recognition of titanite occurrences at Gabal El-Degheimi area, Central Eastern Desert, Egypt, Egypt. J. Remote Sensing Space Sci. (2016), http://dx.doi.org/10.1016/j.ejrs.2016.08.003

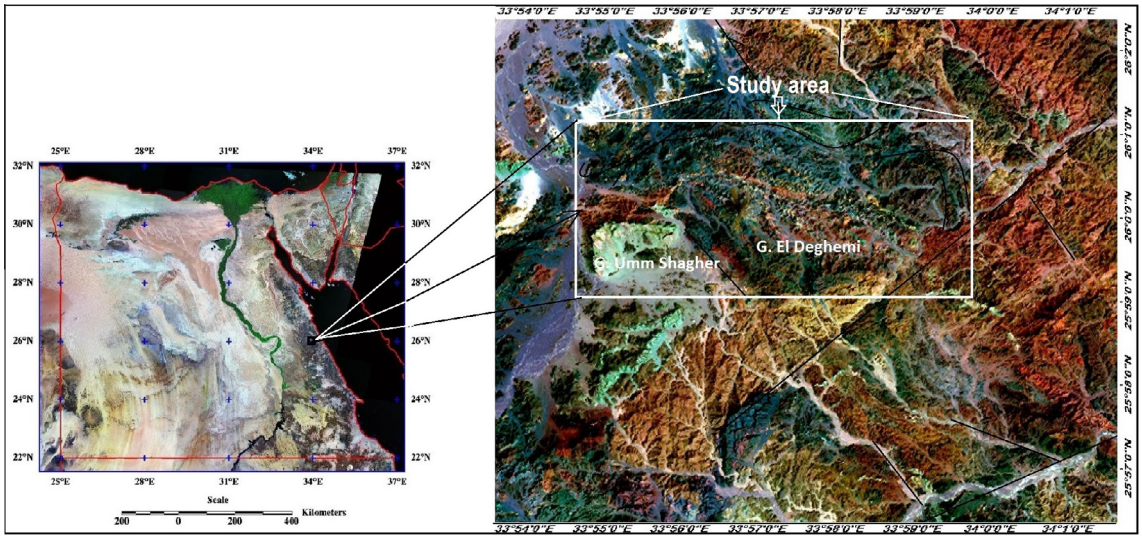


**Figure 1** Left, location map, and right white box, general view of geological and structural features of the study area related to surroundings.

terizes a specific mineral or group of minerals, which is determined by a specific genesis. Volcaniclastic metasediments cover vast areas in the Central Eastern Desert; they develop considerable thicknesses and include metamudstone, greywacke and conglomerate, and are mapped by some authors as titanite-bearing rocks. Moharram et al. (1970) mentioned some mineral deposits in the Central Eastern Desert including titanite at Gabal El-Degheimi area. Hussein (1990) recorded titanite in the metavolcaniclastic at the Umm Shagir- El Degheimi area. The Egyptian geological survey and mining authority (EGSMA, 1997, 1998) studied the mines and quarries in the Central Eastern Desert and recorded titanite in the metavolcanics. Bernau and Franz (1987) studied the crystal chemistry and genesis of Nb-, V- and Al-rich metamorphic titanite from Egypt and Greece. They noticed that titanite from calc-silicate rocks of Gabal Umm Shagir Egypt (included in the study area) is associated with garnet, pyroxene, scapolite, calcite and quartz containing up to 11.0 wt% $Nb_2O_3$, 6 wt% $Al_2O_3$ and 2% $V_2O_5$. Other elements such as Fe, Ta, Sn, and F are present. Piccoli et al. (2000) noticed that Rare Earth Element concentrations generally decrease toward the edge of titanite crystals. However, some crystals are reversely zoned, and others exhibit oscillatory or patchy zoning; some grains contain discrete anhedral cores. Che et al. (2013) grouped the chemical compositions of titanite on the basis of its genesis into: magmatic titanite from igneous rocks, hydrothermal titanite from igneous rocks and hydrothermal veins, metasomatic titanite from skarn samples, and metamorphic titanite from hornfels samples. Major- and trace-element compositions of titanites from representative Cu-mineralized intrusions determined by LA-ICP-MS show higher values for $Fe_2O_3/Al_2O_3$, ΣREE + Y, LREE/HREE, $Ce/Ce^*$, $(Ce/Ce^*)/(Eu/Eu^*)$, U, Th, Ta, Nb and Ga, and lower values for $Al_2O_3$, CaO, $Eu/Eu^*$, Zr/Hf, Nb/Ta and Sr than those for titanites from barren intrusions in the Jinshajiang – Red River alkaline igneous belt, SW China, Xu et al. (2015).

The origin of titanite, partly associated with ilmenite by breakdown of biotite could be described by the following reaction (René, 2010):

-Ca-plagioclase + Biotite + 4 $H_2O$ = Titanite + Ilmenite + Muscovite

Often this alteration is accompanied by sericitization and argillization of plagioclase. The origin of secondary titanite is common in igneous and metamorphic rocks and has been studied in detail by Piccoli et al. (2000), Ciesielczuk and Janeczek (2004), and Broska et al. (2007). Some of the secondary titanites are enriched in Al (Janeczek, 1994; Ciesielczuk and Janeczek, 2004; Broska et al., 2007).

The widespread of volcaniclastic metasediments in the study area with their potentiality in titanite bearing minerals is the main reason which led the authors to undertake the present study.

The aim of the present study is to explore the titanite and explain its mineral chemistry in the host volcaniclastic metasediments at Gabal El-Degheimi area. So, mapping the distribution and occurrences of the volcaniclastic metasediments in relation with surrounding country rocks will clarify and contribute the potentiality of the titanite in the study area.

## 2. Geological setting

The proposed new classification of the Eastern desert basement rocks by Johnson et al. (2011) is quite correlated with the geological setting of the study area. Geology of the study area reflects a small picture of the general geology of the Central Eastern Desert as it includes lots of rock varieties from Proterozoic to late Proterozoic ages. The exposed rocks from the oldest to youngest are as follows; serpentinites, arc volcaniclastic metasediments, older granites, Dokhan volcanics, Hammamat group, post orogenic volcanics and younger granites (Fig. 2). The serpentinites–talc-carbonates encountered in the central parts of the north and south banks of Wadi El-

Please cite this article in press as: Khalil, A.E. et al., Contribution of remote sensing techniques to the recognition of titanite occurrences at Gabal El-Degheimi area, Central Eastern Desert, Egypt, Egypt. J. Remote Sensing Space Sci. (2016), http://dx.doi.org/10.1016/j.ejrs.2016.08.003

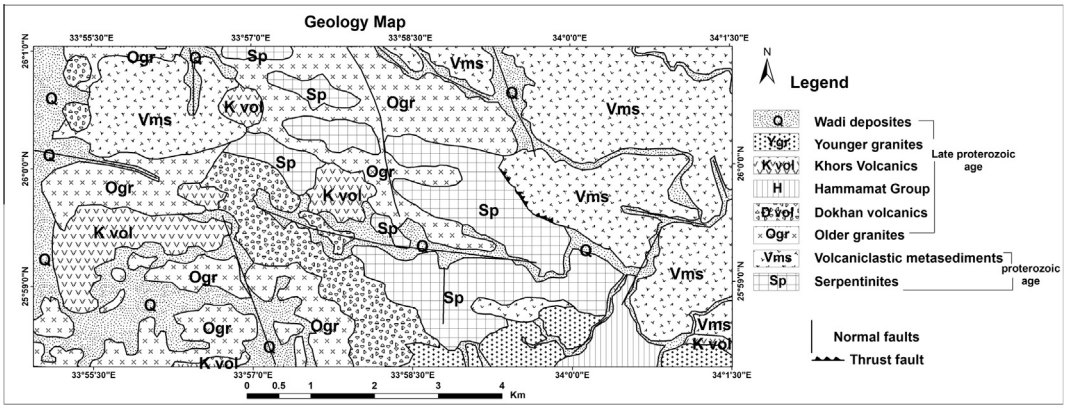


**Figure 2** Geological map of the study area (modified after Akaad and Noweir, 1980).

Hammariya (Khalil, 2000). These constitute exposures of elongated masses extending in a NW–SE trend; some appear thrusting over the volcaniclastic metasediments and others are intruded by the older granites. The volcaniclastic metasediments (biotite–quartz schist) are extended for many kilometers and are interbedded with metagreywackes, metamudstones and metaconglomerates. The schistosity is parallel to the original bedding, intruded by older granites. The coarse varieties (particularly the metaconglomerates) are frequently intercalated with banded iron oxides and volcanic detritus. The wide compositional range of the volcaniclastic metasediments resulting from the metamorphism process and/or the action of mineral bearing hydrothermal solutions which were associated with the intrusions and extrusions of the plutonics and volcanics were favorable for titanite mineral occurrences in these rocks. The older granites include tonalite-granodiorite rocks distributed in the northern parts of the area and including xenoliths of different sizes in the form of serpentinites. The younger granites comprise mixed suites of monzogranite to alkali-feldspar granite emplaced in the south of the area, intruding the Hammamat group. Dokhan and post orogenic Khors volcanics are extruded all the rock varieties as dykes and plugs. The Hammamat molasse sediments were intra-basins deposited contemporaneous to these extrusions in the southeastern corner of the area.

## 3. Methodology

Processing of Landsat 8 (LOI) images verified by field geology supported by analytical techniques (petrography, electron microprobe chemical analyses) were used to achieve and accomplish the desired goals and results of this research.

### *3.1. Remote sensing techniques*

The Landsat 8 (LOI) scene covering the study area was acquired in May 2014. It has been pre-processed and prepared for data extraction by geometry and radiometry correction as well as noise removing and UTM geo-referencing. Image processing approaches were performed using the ERDAS imagines 8.7 and Envi software for geological, lithological and mineralogical identification. The performed image processing included false-color composite (FCC), principal component analysis (PCAs) and band ratios in the red green blue (RGB) because they contain most of the information about the geological features focused in this study. PCA and different tested band ratios are useful for the qualitative detection of hydrothermal alteration minerals and are widely applied in geological and mineral mapping in the Eastern Desert of Egypt (e.g., Di Tommaso and Rubinstein, 2007). The USGS spectral library (http://www.speclab.cr.usgs.gov) of rock forming minerals was used to evaluate the spectral signatures of the identified mineral composition of the different lithological units in the study area. Arc GIS version 10 was used for generating the processed images.

### *3.2. Field geology and sampling*

Based on the remote-sensing data and interpretation of the EGSMA geological map (1997), the field geology was undertaken to verify the remote sensing results in the study area. Representative samples from the volcaniclastic metasediments (the host titanite rock) were collected for analytical techniques.

### *3.3. Analytical techniques*

Petrographic and ore microscopic studies as well as electron microprobe analysis were applied on eight samples collected from the volcaniclastic metasediments in the northern parts of the study area (Fig. 3). As electron microprobes are suitable instruments for quantitative chemical analysis of micro volumes down to 1-2#Lm3, a CAMECA SX50 microprobe under operating conditions of 15 kV accelerating voltage and 15–16 nA sample current measured on Faraday cage and 1–2 μm beam size; element peaks and backgrounds were each measured over 20 s/synthetic silicate and oxide minerals were used for reference standards. The electron microprobe analyses were carried out on 79 spots in different representative minerals in eight selected samples at Würzburg University, Germany to clarify the content and the mineral chemistry of the titanite mineral. In this respect a CAMECA SX-50 instrument was used as an acceleration potential of 20 kV, and a beam current

Please cite this article in press as: Khalil, A.E. et al., Contribution of remote sensing techniques to the recognition of titanite occurrences at Gabal El-Degheimi area, Central Eastern Desert, Egypt, Egypt. J. Remote Sensing Space Sci. (2016), http://dx.doi.org/10.1016/j.ejrs.2016.08.003

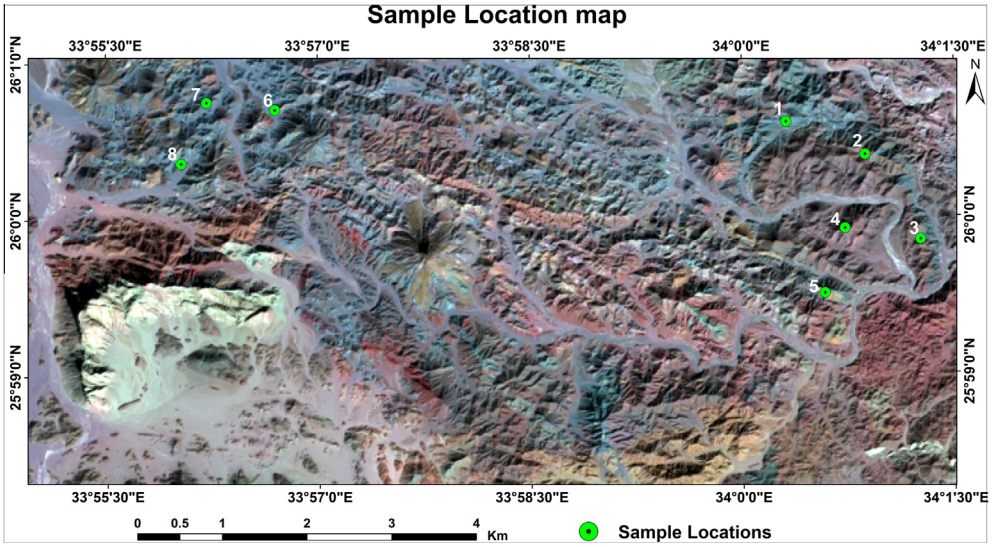


**Figure 3** Location map of electro microprobe analyzed samples from the study area.

of 20 nA. The counting times were 20 s on TAP–PET and 30 s on LiF crystals. Data reduction was made using a CAMECA version of the PAP (Pouchou and Pichoir, 1984) routine.

## 4. Results

### *4.1. Interpretation of the processed Landsat 8*

#### *4.1.1. FCC*

The FCC image bands 7, 5, 3 in RGB give a good view of geological and structure features as well as clear contrast and tracing for the different rocks. In such images the distribution of the rock units were discriminated at different tones due to the specific spectral signatures of each rock. The serpentinites show mottled brown purple color in a thrust contact with the volcaniclastic metasediments, which appear as dull mixed dark green, dark gray to bluish-green and brown colors. Specifically, the younger granitic rocks (mottled greenish yellow color) were differentiated from the older granites (brown to deep brown). See the legend for other rocks (Fig. 4). The image also displayed the normal and thrust faults affecting the rock units.

#### *4.1.2. PCA*

In the image PC2, PC1, PC4 the younger Khors volcanics in the southwest and southeast appear as red color. This image also differentiated between the younger granitic rocks (bright green color) in the south and the older granites (dark green color) in the west. The normal and thrust faults were also displayed, see (Fig. 5).

#### *4.1.3. Band ratio images*

In the processed image after band ratios 6/7, 6/2, 4/2 and their combinations in RGB, some rock units were clearly distin-

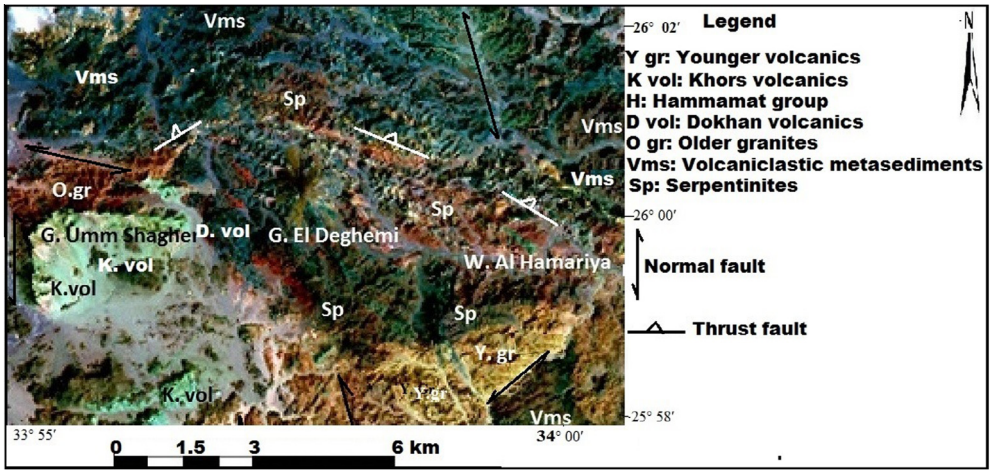


**Figure 4** FCC bands 7, 5, 3 in RGB show the geological and lineament features (NNW–SSE trend) and lithological units in the study area.

Please cite this article in press as: Khalil, A.E. et al., Contribution of remote sensing techniques to the recognition of titanite occurrences at Gabal El-Degheimi area, Central Eastern Desert, Egypt, Egypt. J. Remote Sensing Space Sci. (2016), http://dx.doi.org/10.1016/j.ejrs.2016.08.003

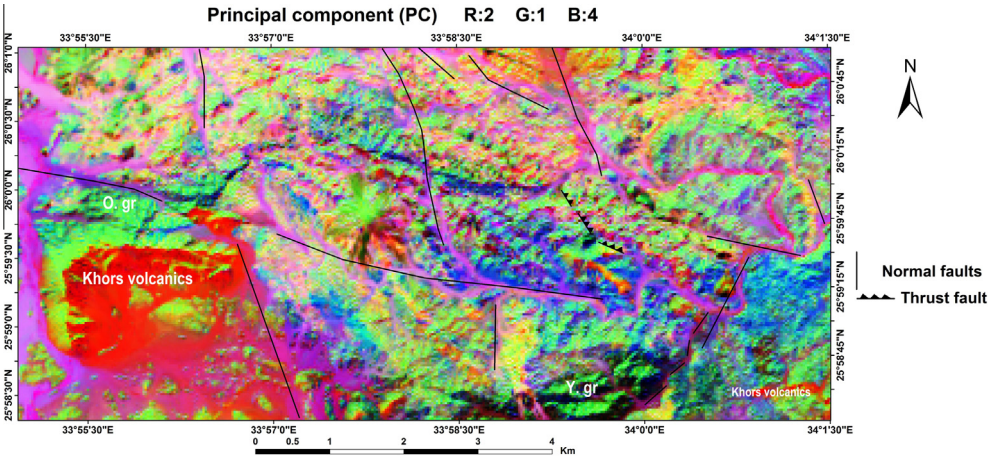


**Figure 5** PCA (PC2, PC1, PC4) of the study area recognized the younger Khors volcanics and older and younger granites.

guished; the volcaniclastic metasediments appear in variable color associations from mottled red green, red yellowish green to blue colors. These mixtures and color differences may be due to the wide range of mineralogical composition of these rocks and of the hosting alteration zones. As so, the serpentinite rocks display color associations that vary from pink, purple to pale blue colors, due to the presence of altered talc carbonates and talc chlorite associations in the serpentinite rocks. The younger Khors volcanic, in the southwest and southeast of the area, shows uniform bright green color, reflecting homogeneity in mineral composition (Fig. 6).

### 4.2. Interpretation of the field geology

The field geological observations revealed the variations in the volcaniclastic metasediments, where the volcanic type varies from rhyolitic to andesitic composition and related pyroclastics. It also revealed the presence of alteration zones in the volcaniclastic metasediments (probably rich in titanite minerals). Also, the younger granites were distinguished from the older ones. The study area comprises huge belt of thick sequence of serpentinites and arc volcaniclastic metasediments extending along a NNW-SSE trend. The sequence is exposed at Wadi Umm Qarati, Wadi Tallet Al-Sheikh together with the various tributaries of Wadi Sodmein. The volcaniclastic metasediments bearing titanite mineral are represented by titanite–biotite–quartz schist, bounded from the north by granodiorite to monzogranite along Wadi Al-Himeiyir and Kab Al-Awazim.

### 4.3. Mineralogy and mineral chemistry

#### 4.3.1. Mineralogy

The volcaniclastic metasediments consist of quartz, K feldspars, Plagioclase, biotite, muscovite and titanite as main minerals, together with minor chlorite, calcite and iron oxides as well as Kaolinite, sericite, saussurite and epidote present as secondary minerals. Quartz is normally found as large xenomorphic clear crystals, it constitutes up to 45% of the mineral constituents of the schists. Plagioclase is found as medium to fine-grained subidiomorphic tabular crystals, strongly saussuritized and untwined and completely masked, displaced and corroded due to alteration. Titanite is light yellow to dark brown in color (Fig. 7a), idiomorphic to subidiomorphic in crystal shape and large in grain size (0.3–0.9 mm, Fig. 7b), it

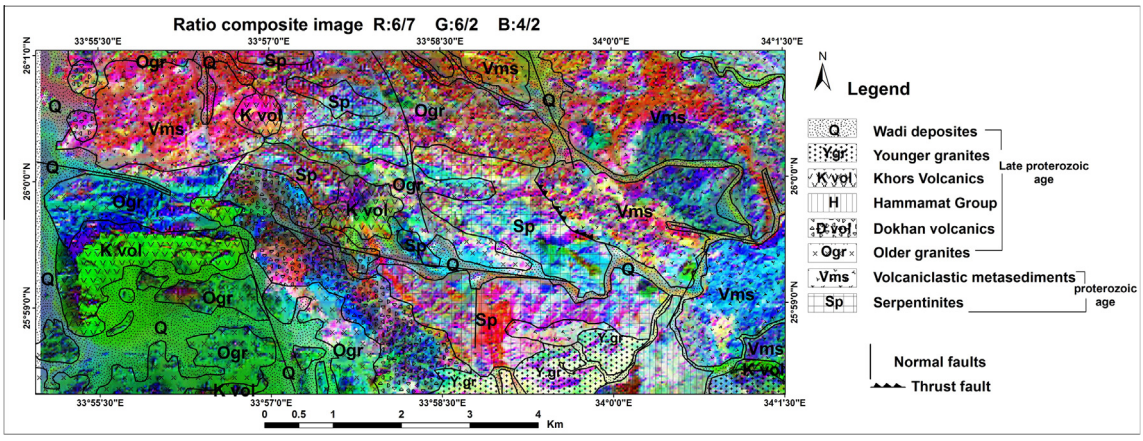


**Figure 6** Band ratios 6/7, 6/2, 4/2 image in RGB, showing some units in numerous (variable) color associations in the study area.

Please cite this article in press as: Khalil, A.E. et al., Contribution of remote sensing techniques to the recognition of titanite occurrences at Gabal El-Degheimi area, Central Eastern Desert, Egypt, Egypt. J. Remote Sensing Space Sci. (2016), http://dx.doi.org/10.1016/j.ejrs.2016.08.003

is usually associated with black iron oxides (Fig. 7c). As observed in thin sections, apatite is commonly embraced by titanite (Fig. 7d). Biotite forms brownish and reddish brown elongate flakes with preferred orientation, being associated with subordinate muscovite and intergrown with quartz. Epidote forms yellowish brown granular aggregates and xenomorphic crystals accompanied with minor titanite and shows high interference colors under Cross Nicols. Apatite appears as granules and/or stout crystals enclosed within the titanite and plagioclase. Iron oxides are present as xenomorphic crystals up to 0.3 mm in size. It is associated with biotite flakes and titanite.

*4.3.2. Mineral assemblages and chemistry and of titanite mineral*

The result of microprobe analyzed samples from the study area is listed in Table 1. There is no clear variation in the titanite compositions, only a decrease in $Al_2O_3$ is associated by an increase in FeO content in samples no (2, 6, 8). CaO content increases proportionally to $TiO_2$ increase, (2). The lowest $TiO_2$ content is reversely proportional to the $FeO^t$ and $SiO_2$ increase, (1). $SiO_2$ decreases with the decreasing of CaO content, (2, 6, 8) Table 1. The averages chemical composition of Gabal El-Degheimi titanite compared to published chemical composition of four titanite samples (from Srilanka and Brazil) are given in Table 2. In which the element oxides, CaO (25.87–27.62 wt%), $SiO_2$ (28.57–29.38 wt%) and $TiO_2$ (35.27–37.21 wt%) exhibit comparatively lower contents than the Srilanka and Brazil titanite. The studied Gabal Degheimi titanite is richer in FeO and very poor in $Al_2O_3$ compared to those of Srilanka and Brazil titanite given in Zwaan and Arps (1980). $Al_2O_3$ varies from 0.83 to1.31 wt% and correlates negatively with $TiO_2$ which also negatively correlates with FeO that is always between 1.41 and 2.19 wt%. The composition of titanite from the examined volcaniclastic metasediments ranges from 80 to 85 mol titanite end-member. Although the composition of titanite from Gabal Degheimi is similar in many

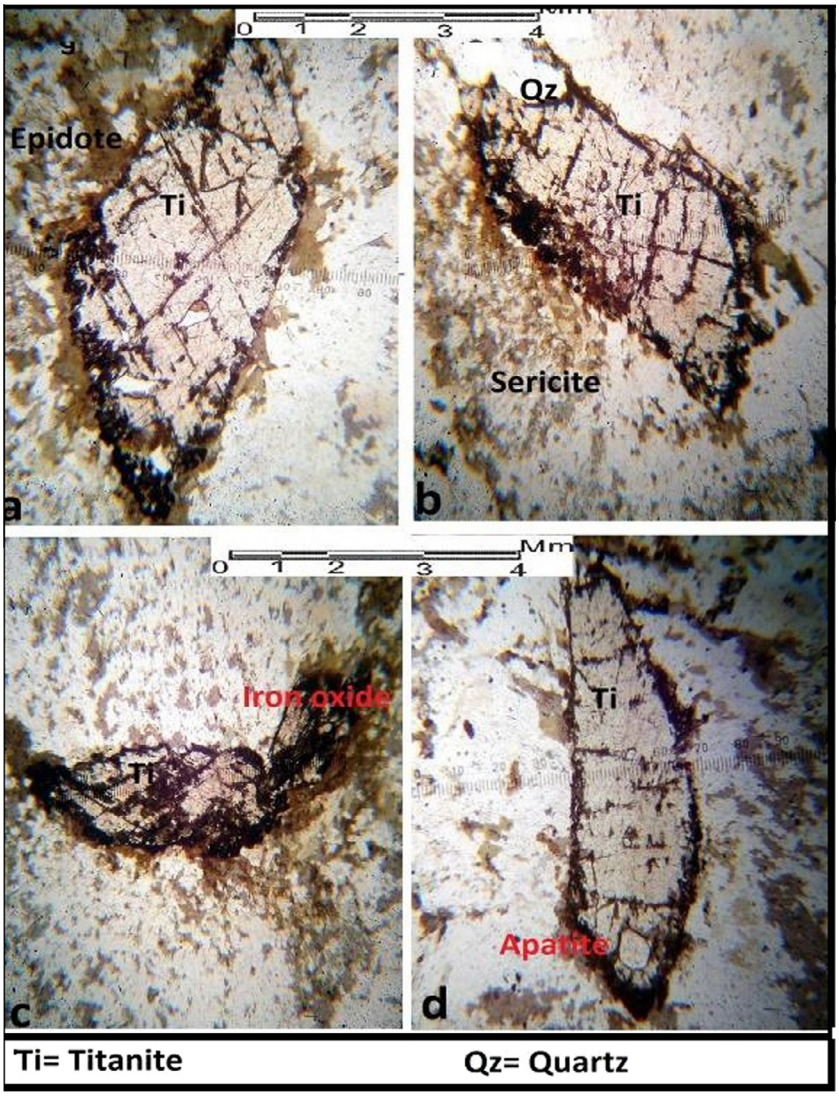


**Figure 7** (a)–(d) Photomicrograph showing petrographical features, all in (PPL). (a)Light brown titanite. (b) Subidiomorphic titanite crystal. (c)Titanite is usually associated with black iron oxides. (d) Apatite is commonly embraced by titanite.

Please cite this article in press as: Khalil, A.E. et al., Contribution of remote sensing techniques to the recognition of titanite occurrences at Gabal El-Degheimi area, Central Eastern Desert, Egypt, Egypt. J. Remote Sensing Space Sci. (2016), http://dx.doi.org/10.1016/j.ejrs.2016.08.003

**Table 1** Electron Probe Micro Analysis Data for elements determined as oxide % on titanite from Gabal Degheimi volcaniclastic metasediments.

| Oxides | 1SP | 2SP | 3SP | 4SP | 5SP | 6SP | 7SP | 8SP |
|---|---|---|---|---|---|---|---|---|
| Symbols | ○ | □ | ■ | + | × | ▲ | ● | △ |
| $SiO_2$ | 29.21 | 29.18 | 29.03 | 28.57 | 28.98 | 28.86 | 29.02 | 29.38 |
| CaO | 26.33 | 27.62 | 26.90 | 25.87 | 26.17 | 26.57 | 27.17 | 27.21 |
| $FeO^{total}$ | 2.19 | 1.48 | 1.65 | 1.77 | 1.94 | 1.63 | 1.73 | 1.41 |
| $Al_2O_3$ | 1.31 | 0.93 | 1.07 | 1.01 | 1.11 | 0.83 | 1.07 | 0.97 |
| $TiO_2$ | 35.27 | 37.21 | 36.54 | 36.05 | 35.32 | 36.28 | 36.26 | 36.88 |
| *Unit cell contents on the basis of 19 O* | | | | | | | | |
| Si | 3.66 | 3.58 | 3.60 | 3.61 | 3.65 | 3.62 | 3.60 | 3.62 |
| Ca | 3.53 | 3.63 | 3.58 | 3.51 | 3.53 | 3.57 | 3.61 | 3.59 |
| $Fe^2$ | 0.23 | 0.15 | 0.17 | 0.19 | 0.21 | 0.17 | 0.18 | 0.15 |
| Al | 0.19 | 0.13 | 0.16 | 0.15 | 0.18 | 0.12 | 0.16 | 0.14 |
| Ti | 3.32 | 3.43 | 3.41 | 3.43 | 3.35 | 3.42 | 3.38 | 3.41 |

**Table 2** Average chemical composition of Gabal El-Degheimi titanite, compared to international published analyzed samples.

| Oxides | 1 | 2 | 3 | 4 | 5 |
|---|---|---|---|---|---|
| CaO | 26.81 | 28.55 | 28.70 | 28.57 | 27.96 |
| $TiO_2$ | 36.23 | 38.5 | 38.50 | 39.43 | 30.39 |
| $Al_2O_3$ | 1.04 | 1.18 | 1.00 | 0.09 | 4.93 |
| $FeO^{total}$ | 1.73 | 0.65 | 0.66 | 1.14 | 2.92 |
| $SiO_2$ | 29.03 | 30.40 | 30.40 | 30.61 | 30.75 |
| *Unit cell contents on the basis of 4 O* | | | | | |
| Ca | 3.57 | 3.77 | 3.73 | – | – |
| Ti | 3.39 | 3.61 | 3.64 | – | – |
| Al | 0.15 | 0.18 | 0.15 | – | – |
| $Fe^2$ | 0.18 | 0.07 | 0.06 | – | – |
| Si | 3.62 | 3.80 | 3.82 | – | – |

(1) Average chemical composition of Gabal El-Degheimi titanite.
(2 & 3) Average chemical composition of Sri Lanka and Brazil titanite (Zwaan and Arps, 1980).
(4) Average chemical composition of Goschener Alp, Switzerland titanite (Dana, 1892).
(5) Average chemical composition of Pierceville, New York, USA titanite (Deer et al., 1982).

aspects to that of the Sri Lanka and Brazil titanite (Table 2) because of similar environments of formation, some significant differences are apparent as follows; a reasonable correlation between Ti and Fe of Gabal-El Degheimi titanite (Fig. 8) is apparent suggesting that in Fe-bearing titanites there is an obvious substitution to consider, i.e. a direct isovalent octahedral substitution Ti ↔ Zr which is different from Sri Lanka and Brazil titanite. Note that the data are shifted below 0.4 line because some Ti is involved in several other cationic exchanges as outlined above. An important point to consider in this regard is that all Fe-bearing titanites so far reported in the mineralogical literature are from high-temperature and alkali-rich volcanic environment; therefore they are of low moderate metamorphic grade.

The mineral assemblages in the volcaniclastic metasediments possibly developed by magmatic segregation in the following way; the volcaniclastic metasediments was deposited together with heavy minerals; zircon, apatite, ilmenite and those that provided Ti. The development of the Ti continued with the formation of an inner rim with increasing proportion of (Al + OH) and decreasing proportion of (Al + $Fe^{+2}$) end members. The inner rim is considered to be the product of mineral reactions involving the previously formed (Al, $Fe^{+2}$)-rich cores and the matrix minerals. The core of the titanite is interpreted as a product of moderate grade metamorphism in which the apatite and iron oxide inclusions are either relics or have formed during the metamorphism from other complex oxides (Zwaan and Arps, 1980). The breakdown of iron oxides leads to titanite compositions more enriched in the CaAl (OH) $SiO_4$ component. The variation of the trace elements observed in titanite is a direct reflection of the compositional zoning pattern. Melts that are enriched in particular trace elements pass on their signature to the titanites.

The crystal chemistry of titanite depends on their crystallochemical properties showing considerable variation in the octahedral sites normally occupied by $Ti^{4+}$ (Ribbe, 1980). The chemical substitutions of the titanite CaTi ($SiO_4$) (O, OH, F), commonly shows considerable isomorphous substitutions (Sahama, 1946; Higgins and Ribbe, 1976; Oberti et al., 1991). More recently, Perseil and Smith (1995) have compiled

Please cite this article in press as: Khalil, A.E. et al., Contribution of remote sensing techniques to the recognition of titanite occurrences at Gabal El-Degheimi area, Central Eastern Desert, Egypt, Egypt. J. Remote Sensing Space Sci. (2016), http://dx.doi.org/10.1016/j.ejrs.2016.08.003

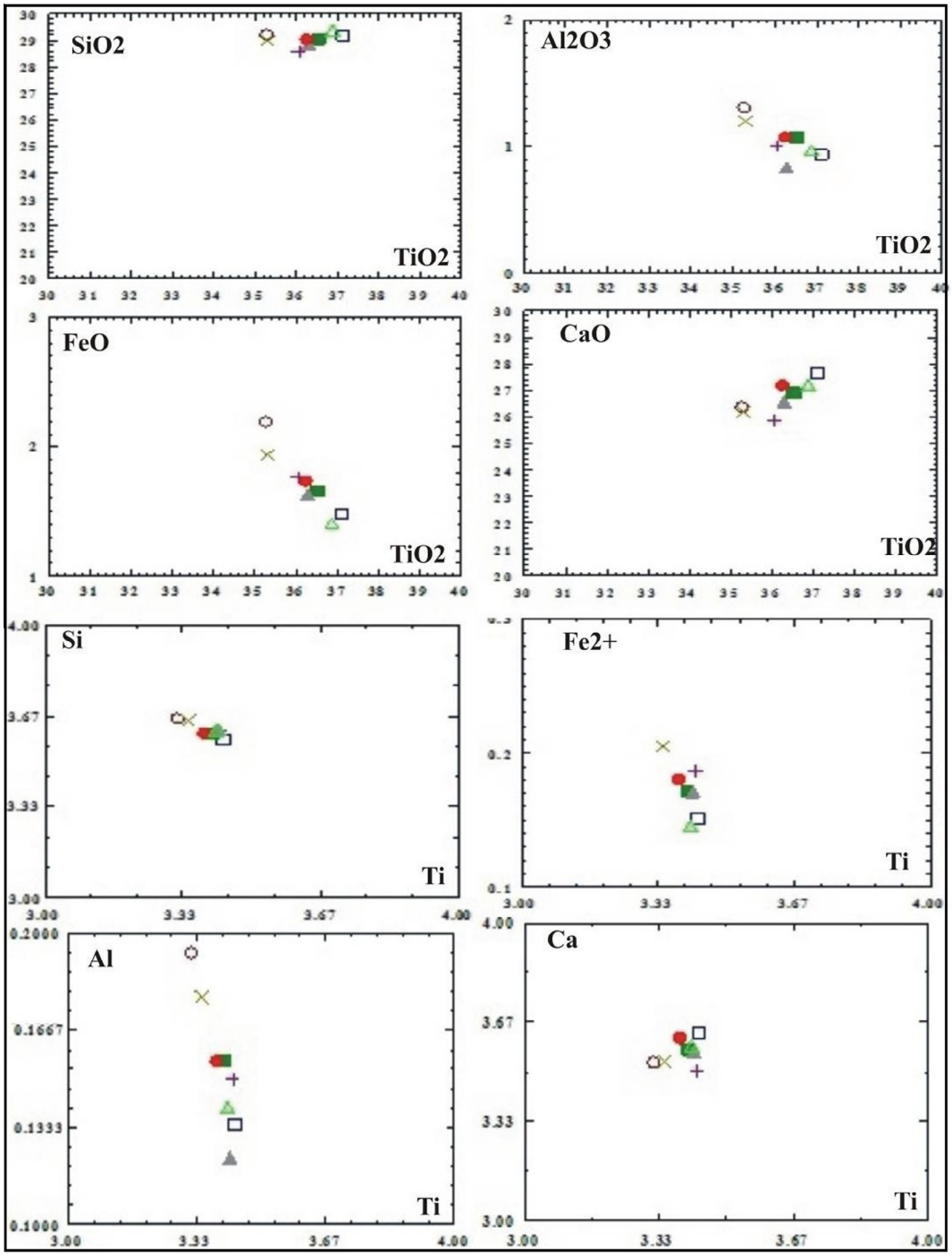


**Figure 8** Variation diagram of $TiO_2$ in relation with other oxides and Ti cation in relation with other cations. Legend is in Table 1.

a list of those elements which can enter the titanite structure and have discussed the various possible substitution schemes, the most important being:

(i) $(Al, Fe^{3+}) + (OH, F) \leftrightarrow Ti^{4+} + O^{2-}$; is the main mechanism whereby (OH, F) replaces the O oxygen in the structure (Mongiorgi and Riva di Sanseverino, 1968; Isetti and Penco, 1968; Černý and Riva di Sanscverino, 1972; Enami et al., 1993).

(ii) $M^{3+} + (Al, Fe^{3+}) \leftrightarrow Ca^{2+} + Ti^{4+}$; where trivalent cations ($M^{3+}$), commonly REE, but also Sb (Perseil and Smith, 1995), substitute for Ca.

(iii) $M^{5+} + (Al, Fe^{3+}) \leftrightarrow Ti^{4+}$; where pentavalent cations ($MS^{+}$), notably Nb and Ta (Clark, 1974; Paul et al., 1981; Groat et al., 1985; Russell et al., 1994), are allocated at the octahedral site.

Please cite this article in press as: Khalil, A.E. et al., Contribution of remote sensing techniques to the recognition of titanite occurrences at Gabal El-Degheimi area, Central Eastern Desert, Egypt, Egypt. J. Remote Sensing Space Sci. (2016), http://dx.doi.org/10.1016/j.ejrs.2016.08.003

## 5. Discussion

The previous works on the Eastern Desert of Egypt have pointed to the presence of Titanite mineral in the volcaniclastic metasediments distributed in the Central Eastern parts of this desert. The study area was selected based on the occurrences of these rocks and the influence of the intrusions and extrusions of plutonic and volcanic rocks associated with them and triggering the action of hydrothermal solutions which might constitute an appropriate geological environment to search for titanite mineral. Integrated methods of remote sensing, field geology and chemical analysis were combined and used for the completion of this study.

The examined volcaniclastic metasediments is a part of an island arc suite which was recently considered as a part of the undifferentiated Neoproterozoic basement of the area (Johnson et al., 2011). William (2007) mentioned that the Titanite from the Ross of Mull Granite displays a large variety of textural features, both with respect to crystal shape and compositional zoning. Carlier and Lorand (2008) studied Zr-rich titanite (titanite up to 5.3 wt% $ZrO_2$) and record strong oxidation associated with magma mixing at emitted peraluminous rhyolites and trachydacites and concluded that a late-magmatic oxidation is ascribed to assimilation of water from the felsic melts during magma mixing. Rabbia et al. (2009) studied the mineralogy, texture, and chemical analyses of hydrothermal rutile in the El Teniente porphyry Cu–Mo deposit to constrain the ore formation processes and concluded that rutile formed from igneous sphene, biotite, Ti-magnetite, and ilmenite (Ti-rich phases) by re-equilibration and/or breakdown under hydrothermal conditions at temperatures ranging between 400 °C and 700 °C.

## 6. Conclusions

The used tools led to recognize and discriminate the titanite bearing volcaniclastic metasediments and their relation with surrounding country rock units in various contacts between these units (Fig. 2). The image processing of image bands 7, 5, 3 and band ratios 6/7, 6/2, 4/2 differentiated younger granites from the older granites which were mapped by Akaad and Noweir, 1980 as older granites. The hydrothermally altered zones in the volcaniclastic metasediments are regarded as targets for titanite and associated element occurrences. The study indicates the presence of silicate volcaniclastic metasediments with high content of Ti, Ca, Si and mineralogical attributes with silicate minerals hosting these elements. It may be concluded that the silicate rocks with more exotic geochemistry be available in the Arabian Nubian shield schistose terrains. In that case, the drainage basins of such terrains may be potential areas to be explored for these minerals.

The mineral chemistry of the volcaniclastic metasediments was investigated by electron microprobe and displayed the titanite as a common accessory mineral in this rock and in some skarns. $TiO_2$ content of titanite is about 35.27–37.21 wt %. The larger grains of titanite in volcaniclastic metasediments contain 37.21 wt% of $TiO_2$, 27.62 wt% of CaO and 29.38 wt% of $SiO_2$. These values are comparable to the reported values in Sri Lanka and Brazil titanites. Titanite juxtaposed with ilmenite contain a higher amount of $TiO_2$ about 41–43 wt% much above reported value. The fine grained titanite in volcaniclastic metasediments are of the Ti-enriched ones with a lower amount of $SiO_2$ (28.57 wt%) and a higher amount of CaO (25.87 wt%).

Zoning is very strong and irregular, reflecting growth conditions at different stages of metamorphism.

The magmatic segregation syngenetic origin is the preferred genesis of the titanite mineral occurrence, indicated by the presence of titanite as an accessory mineral formed in the later stage of segregation and/or from the hydrothermal solutions activity in the surrounding volcaniclastic metasediments.

The combined methods have shown compatibility of the results of titanite exploration in the volcaniclastic metasediments. This reflects the need of using multiple ways to obtain confirmatory data and qualified results. Contribution of remote sensing techniques with detailed geological and geochemical mineral exploration for other areas in Eastern Desert and similar regions in the Egyptian deserts and others is recommended.

## Conflict of interest

There is no conflict of interest.

## Acknowledgments

The authors of this work acknowledge the Würzburg University, Germany for its great help in the electron-probe microanalysis for the interpretations of this study.

## References

Akaad, M.K., Noweir, A.M., 1980. Geology and lithostratigraphy of the Arabian Desert orogenic belt of Egypt between latitudes 25°35_N and 26°30_N. Inst. Appl. Geol. Jeddah Bull. 3, 127–135.

Bernau, R., Franz, G., 1987. Crystal chemistry and genesis of Nb-, V- and Al-rich metamorphic titanite from Egypt and Greece. Can. Mineral. 25, 695–705.

Broska, I., Harlov, D., Tropper, P., Siman, P., 2007. Formation of magmatic ilmenite and titanite-ilmenite phase relations during granite alteration in the Tříbeč Mountains, Western Carpathians, Slovakia. Lithos 95, 58–71.

Carlier, G., Lorand, J.P., 2008. Zr-rich accessory minerals (titanite, perrierite, zirconolite, baddeleyite) record strong oxidation associated with magma mixing in the south Peruvian potassic province. Lithos 104 (1), 54–70.

Černý, P., Riva di Sanscverino, L., 1972. Comments on crystal chemistry of titanite. N. Jahrh. Mineral. Monatsh, 97–103.

Che, X.D., Linnen, R.L., Cheng Wang, R., Groat, L.A., Brand, A.A., 2013. Distribution of trace and rare earth elements in titanite from tungsten and molybdenum deposits in Yukon and British Colombia, Canada. Can. Mineral. 51, 415–438.

Ciesielczuk, J., Janeczek, J., 2004. Hydrothermal alteration of the Strzelin granite, SW Poland. N. Jb. Miner. Abh. 179, 239–264.

Clark, A.M., 1974. A tantalum-rich variety of sphene. Mineral. Mag. 39, 60–75.

Dana, E.S., 1892. Dana's system of mineralogy, 6th ed., 712–716, 717 [keilhauite].

Deer, W.A., Howie, R.A., Zussman, J., 1982. Rock-forming minerals, 2nd ed., v. 1A, orthosilicates, 443–466.

Di Tommaso, I., Rubinstein, N., 2007. Hydrothermal alteration mapping using ASTER data in the infernally porphyry deposit, Argentina. Ore Geol. Rev. 32, 275–290.

EGSMA, 1997. Mines and quarries in six years (1990–1996). Egyptian Geological Survey and Mining Authority Cairo Egypt, 133p.

EGSMA, 1997. Geological map of Qift-Quseir Quadrangle, Egypt scale 1:100000. Egyptian Geological Survey and Mining Authority Cairo Egypt.

EGSMA, 1998. Egyptian Geological Survey and Mining Authority in the year 1996–1997. Ministry of Industry and Mineral Resources, Cairo, 84p.

Enami, M., Suzuki, K., Liou, J.G., Bird, D.K., 1993. Al–$Fe^{3+}$ and F–OH constraints on their P–T dependence. Eur. J. Mineral. 5 (219), 31.

Garven, G., Appold, M.S., Toptygina, V.I., Hazlett, T.J., 1999. Hydrogeologic. modeling of the genesis of carbonate-hosted lead–zinc ores. J. Hydrol. 7, 108–126.

Groat, L.A., Carter, R.T., Hawthorne, F.C., Ercit, T.S., 1985. Tantalian niobian titanite from the Irgon Claim, southeastern Manitoba. Can. Mineral. 23 (569), 71.

Higgins, J.B., Ribbe, P.H., 1976. The crystal chemistry and space groups of natural and synthetic titanites. Am. Mineral. 61, 878–888.

Hussein, A.A., 1990. Mineral deposits. In: Said, R., Balkema, A.A. (eds.), The Geology of Egypt. Rotterdam.

Isetti, G., Penco, A.M., 1968. La posizione dell'idrogeno ossidrilico nella titanite. Mineral. Petrogr. Acta 14, 115–122.

Janeczek, J., 1994. The effect of aluminous titanite on the biotite–chlorite and amphibole–chlorite reactions. Eur. J. Mineral. 6, 623–625.

Johnson, P.R., Andresen, A., Collins, A.S., Fowler, A.R., Fritz, H., Ghebreab, W., Kusky, T., Stern, R.J., 2011. Late Cryogenian-Ediacaran history of the Arabian-Nubian Shield: a review of depositional, plutonic, structural, and tectonic events in the closing stages of the northern East African Orogen. J. Afr. Earth Sci. 61, 167–232.

Khalil, A.E., 2000. Petrological and Geochemical Studies on the Serpentinites of Umm Saneyat, El-Deigheimi and El-Muweilih Areas, Qift-Quseir Road, Eastern Desert, Egypt (Ph.D. thesis). Faculty of Science, Al-Azhar University, Egypt, pp. 181–200.

Moharram, O., El Ramly, M.F., Amer, A.F, Gachechiladze, D.Z., Ivanov, S.S., 1970. Studies on some mineral deposits of Egypt. Geological Survey of Egypt, Cairo.

Mongiorgi, R., Riva di Sanseverino, L., 1968. A reconsideration of the structure of titanite, $CaTiOSiO_4$. Mineral. Petrogr. Acta 14, 123–141.

Nesbitt, B.E., 1992. Orogeny crustal hydrogeology and the generation of epigenetic ore deposits in the Canadian Cordillera. Mineral. Petrol. 45, 153–179.

Oberti, R., Smith, D.C., Rossi, G., Caucia, F., 1991. The crystal-chemistry of high-aluminium titanites. Eur. J. Mineral. 3, 777–792.

Oliver, J., 1986. Fluids expelled horizontally from orogenic belts: their role in hydrocarbon migration and other geologic phenomena. Geology 14, 99–102.

Paul, B.J., Černý, P., Chapman, R., Hinthome, L.R., 1981. Niobian titanite from the Huron Claim pegmatite, southeastern Manitoba. Can. Mineral. 19 (549), 52.

Perseil, E., Smith, D.C., 1995. Sb-rich titanite in the manganese concentrations at St. Marcel-Praborna, Aosta Valley, Italy: petrography and crystal chemistry. Mineral. Mug 59, 717 34.

Piccoli, P., Candela, P., Rivers, M., 2000. Interpreting magmatic processes from accessory phases: titanite – a small-scale recorder of large-scale processes. Geol. Soc. Am. Spec. Pap. 350, 257–267.

Pouchou, F., Pichoir, J. Microsc., 1984. Possibilités d'analyse en profondeur à la microsonde électronique. Spectrosc. Electron 9, 99–100.

Rabbia, O.M., Hernández, L.B., French, D.H., King, R.W., Ayers, J. C., 2009. The El Teniente porphyry Cu–Mo deposit from a hydrothermal rutile perspective. Miner. Deposita 44 (8), 849–866.

René, M., 2010. Titanite–ilmenite assemblage in Redwitzites of the Slavkovský Les Mts. (Bohemian Massif, Czech Republic). Acta Geodyn. Geomater. 7 (4), 445–452.

Ribbe, P.H., 1980. Titanite (sphene). Ch. 6 in Orthosilicates. In: Ribbe, P.H., ed., Reviews in Mineralogy, vol. 5, 137–154.

Russell, J.K., Groat, L.A., Halleran, A.A.D., 1994. LREE-rich niobian titanite from Mount Bisson, British Columbia: chemistry and exchange mechanisms. Can. Mineral. 32 (575), 87.

Sahama, Th.G., 1946. On the chemistry of the mineral titanite. Bull. Comm. Geol. Finlande 138 (88), 120.

USGS spectral library (http://www.speclab.cr.usgs.gov).

William, G., 2007. Titanite Zoning and Magma Mixing (Ph.D. thesis). Department of Geographical & Earth Science, Glasgow University.

Xu, Leiluo, Bi, Xianwu, Hu, Ruizhong, Tang, Yongyong, Wang, Xinsong, Xu, Yue, 2015. LA-ICP-MS mineral chemistry of titanite and the geological implications for exploration of porphyry Cu deposits in the Jinshajiang – Red River alkaline igneous belt, SW China. Mineral. Petrol. 109 (2), 181–200.

Zwaan, P.C., Arps, C.E.S., 1980. Sphene, Sri Lanka's newest gemstone. Scripta Geol. 58.

Please cite this article in press as: Khalil, A.E. et al., Contribution of remote sensing techniques to the recognition of titanite occurrences at Gabal El-Degheimi area, Central Eastern Desert, Egypt, Egypt. J. Remote Sensing Space Sci. (2016), http://dx.doi.org/10.1016/j.ejrs.2016.08.003